Hindawi
Journal of Control Science and Engineering
Volume 2023, Article ID 9792786, 1 page
https://doi.org/10.1155/2023/9792786

Retraction

Retracted: Application of CAD Technology in Extracting Line Feature of Industrial Part Image

Journal of Control Science and Engineering

Received 17 October 2023; Accepted 17 October 2023; Published 18 October 2023

This article has been retracted by Hindawi following an investigation undertaken by the publisher [1]. This investigation has uncovered evidence of one or more of the following indicators of systematic manipulation of the publication process:

(1) Discrepancies in scope
(2) Discrepancies in the description of the research reported
(3) Discrepancies between the availability of data and the research described
(4) Inappropriate citations
(5) Incoherent, meaningless and/or irrelevant content included in the article
(6) Peer-review manipulation

The presence of these indicators undermines our confidence in the integrity of the article's content and we cannot, therefore, vouch for its reliability. Please note that this notice is intended solely to alert readers that the content of this article is unreliable. We have not investigated whether authors were aware of or involved in the systematic manipulation of the publication process.

Wiley and Hindawi regrets that the usual quality checks did not identify these issues before publication and have since put additional measures in place to safeguard research integrity.

We wish to credit our own Research Integrity and Research Publishing teams and anonymous and named external researchers and research integrity experts for contributing to this investigation.

The corresponding author, as the representative of all authors, has been given the opportunity to register their agreement or disagreement to this retraction. We have kept a record of any response received.

References

[1] F. Li, "Application of CAD Technology in Extracting Line Feature of Industrial Part Image," *Journal of Control Science and Engineering*, vol. 2022, Article ID 6372168, 8 pages, 2022.

Hindawi
Journal of Control Science and Engineering
Volume 2022, Article ID 6372168, 8 pages
https://doi.org/10.1155/2022/6372168

Research Article

Application of CAD Technology in Extracting Line Feature of Industrial Part Image

Fei Li

Huaibei Vocational and Technical College of Arts and Crafts Department, Huaibei 235000, Anhui, China

Correspondence should be addressed to Fei Li; 20150235122@mail.sdufe.edu.cn

Received 21 July 2022; Revised 2 September 2022; Accepted 10 September 2022; Published 24 September 2022

Academic Editor: Jackrit Suthakorn

In order to solve the problem that the properties of the acquired images in engineering are often poor and the features of the images are seriously lost, so that the image features cannot be effectively developed, an application method of CAD technology in the extraction of linear features of industrial parts images is proposed. Based on 3D computer-aided design (CAD) data, by solving the parameter transformation relationship between the CAD 3D Cartesian coordinate system and the image coordinate system, the target line feature is projected onto the image, and the initial value range of the image line feature is obtained. The edge point sequence is extracted by multiplication template matching, and the generated point sequence is fitted by the least square method to obtain the line equation of the image line feature. By solving the intersection of the intersecting lines of the image, the straight line segment representing the contour of the industrial part can be obtained with high precision. The experimental results show that the above algorithm is used to extract the line features of real industrial part images, and the median error of the difference between the reconstructed line length and the line length measured by the vernier caliper is 0.232 mm. The practice has proved that CAD technology has a certain auxiliary and guiding role in the research of industrial part image feature extraction algorithms. It can be applied to high-precision image measurement and reverse engineering of regular industrial parts. In engineering technology, it can help improve the automation level of industrial production.

1. Introduction

The line feature in the image is an important clue for visual perception and the basic basis for interpreting the image. It often corresponds to the outline or boundary line of the subject and is the "meaningful" change in the image; at the same time, the line feature is the rule. Objects, especially man-made objects, are one of the basic elements. Beginning in the mid-1990s, 3D shape models have been widely used in various fields, including industrial design, computer simulation, architectural design, virtual reality, molecular biology, education, 3D animation, fashion design, film and television works, and historical and cultural protection. With the large-scale growth of 3D shape models, 3D shape retrieval technology emerges as the times require. It solves the problem of the reuse of 3D shape models with similar shape features and has become a research hotspot after text retrieval, image retrieval, video retrieval, artificial intelligence, computer vision, pattern recognition, and other fields. 3D shape retrieval mainly includes the following three steps: preprocessing, 3D shape feature extraction, and similarity comparison [1]. As the core technology of 3D shape retrieval, the research of 3D shape feature extraction technology has been a research hotspot in recent years. The quality of 3D shape feature extraction technology determines whether the feature information can accurately express a unique 3D shape, which directly affects the accuracy of 3D shape retrieval. With the wide application of 3D shapes and the increase of 3D shape libraries on the Internet, many existing 3D shapes have strong variability, especially in 3D shapes with hinges, joints, and other structures, such as human bodies, animals, and toys. When such three-dimensional shapes are subjected to a certain degree of rigid or isometric transformations, rigid deformation will occur, so that the shape feature descriptors of the same shape after deformation are very different. The traditional feature

extraction technology is not suitable for processing 3D models with an increasingly large amount of data and increasingly complicated structural features. For industrial CAD 3D shapes or 3D shapes with hole and cavity structures, the extraction results are not ideal and the practicability is not strong, which is also the current 3D model. The shape feature extraction technology needs to be improved [2, 3]. Figure 1 shows the basis of computer-aided design creation. Feature extraction is a concept in computer vision and image processing. It refers to using a computer to extract image information to decide whether each image point belongs to an image feature. The result of feature extraction is to divide the points on the image into different subsets, which often belong to isolated points, continuous curves, or continuous regions. Feature extraction is a primary operation in image processing, that is to say, it is the first operation to process an image. It examines each pixel to determine whether the pixel represents a feature. If it is part of a larger algorithm, then the algorithm generally only examines characteristic regions of the image. As a prerequisite for feature extraction, the input image is typically smoothed in scale space by a Gaussian blur kernel. One or more features of the image are then computed through local derivative operations.

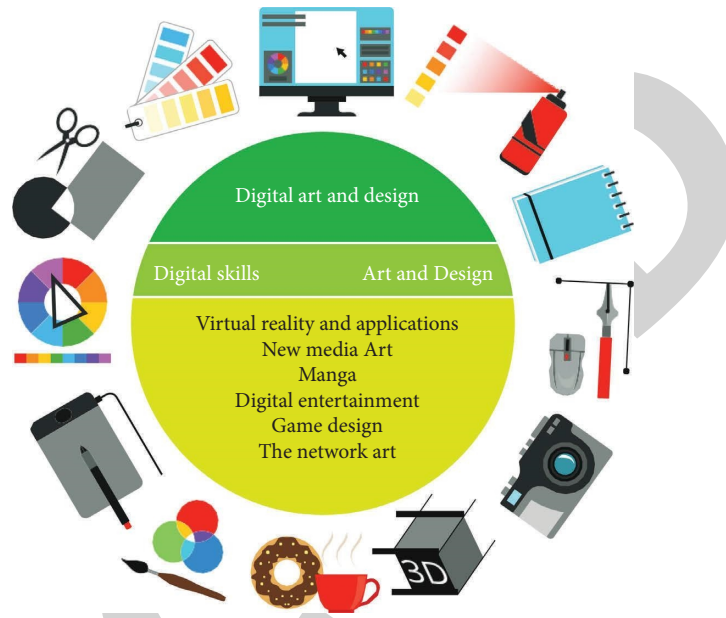

Figure 1: The basis of computer-aided design creation.

2. Literature Review

Gao and Bhagi proposed basic surface features including D2 (point-to-point distance distribution), surface normal, chord angle, and a linear combination of length, curvature, and volume distribution. Among them, the D2 signature can be computed quickly, and it is insensitive to rotation, translation, scaling, simplification, and model degradation. For simple models, such as circles, triangles, cubes, and spheres, the method performs well, but for complex models, the shape distribution D2 tends to be a bell-shaped normal distribution. As a result, it can classify two completely different models into the same class [4]. Ignaczak et al. proposed the spectral shape distance, a distribution based on the general diffusion distance. Diffusion metrics contain a lot of geometric information about the underlying shape, but a direct comparison of metrics when dealing with two different shape matches is problematic because it needs to deal with the correspondence between the shapes first. There are also methods for model matching based on the density features of points, some works have investigated manifold tools to analyze surface feature density [5]. In Cardaliaguet and Forcadel, the temperature distribution (TD) descriptor is calculated by assigning element heat at each vertex and computing the change in surface temperature distribution over time to represent the shape. The retrieval performance between TD, eigenvalue descriptor (EVD), and D2 descriptor is compared. The result shows that TD descriptors outperform EVD and D2 shape descriptors [6]. Chahi et al. proposed the use of intrinsic distance to construct shape descriptors [7]. The five descriptors proposed by Feng et al. are invariant to rigid transformations, such as translation, selection, and scale, and are robust to noise. Their research experiments show that the geometric shape descriptor D2 is the best among the five shape descriptors. However, 3D models have complex 3D shape information and richer details than 2D images, while a single D2 shape feature describes the 3D shape as very rough [8]. Their work shows that, compared with the non-Euclidean distance, the internal distance is more accurate in describing complex shapes, especially for those structures with joint parts, and it is more effective in describing local structures. In addition, the author proposes three methods to further verify the efficiency of shape classification, namely, methods that consider features such as inner distance itself, the combination of inner distance and multidimensional scaling analysis (MDS), and texture information, respectively.

The author studies the linear feature extraction problem in the image measurement and reconstruction of regular industrial parts. Firstly, according to the CAD three-dimensional design drawing of industrial parts, we establish the object-side CAD rectangular coordinate system by selecting a certain number (at least 6 groups) of two-dimensional and three-dimensional point pairs. Using the principle of least squares, the transformation relationship between the two-dimensional image coordinate system and the three-dimensional object coordinate system is established. Then, by analyzing the DXF file structure of the CAD data, the straight line entity is projected into the image coordinate system (when the straight line segment on the part has the foreground and the background, it needs to be blanked), and the projected value is the initial value range. Within the given initial value range, the line feature template generated by the adaptive method is subjected to least squares template matching along the search window in order to obtain a sequence of line edge points. By eliminating gross errors and setting thresholds, the generated point sequence is fitted with the least squares method, and the straight line equation of the image line features is obtained. By solving the intersection of the intersecting lines of the images, the

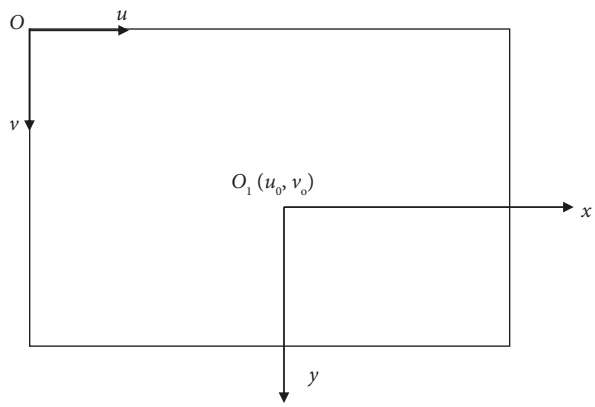

Figure 2: Schematic diagram of the image coordinate system.

straight line segments expressing the contours of industrial parts can be obtained with high precision.

3. Research Methods

3.1. Obtaining the Initial Value

3.1.1. Coordinate System and Its Transformation Relationship. From the camera coordinate system to the image coordinate system, it belongs to the perspective projection relationship and converts from 3D to 2D. The image coordinate system refers to the coordinate system of the digital image stored in the computer, which can be represented by two methods, as shown in Figure 2: (1) expressed in pixel units, the origin of the image coordinate system is in the upper left corner of the image, the positive direction of the u-axis is horizontal to the right, and the positive direction of the v-axis is vertically downward, the units of the u-axis and v-axis are pixels, and (u, v) is used to represent the coordinates of a point in the image coordinate system; (2) expressed in units of length (millimeters, microns, etc.), the origin of this coordinate system is located at the geometric center (u_0, v_0) of the image, the positive direction of the x-axis is horizontal to the right, the positive direction of the y-axis is vertically downward, and (x, y) is used to represent the coordinates of a point in the image coordinate system.

The transformation relationship between the image coordinates of any point and its physical coordinates is as follows [9]:

$$\begin{Bmatrix} u \\ v \\ 1 \end{Bmatrix} = \begin{Bmatrix} \frac{1}{k} & 0 & u_0 \\ 0 & \frac{1}{l} & v_0 \\ 0 & 0 & 1 \end{Bmatrix} \begin{Bmatrix} x \\ y \\ z \end{Bmatrix}. \tag{1}$$

Among them, k and l are the length and width of the pixel respectively, in millimeters.

The camera coordinate system (X_c, Y_c, Z_c) refers to a three-dimensional rectangular coordinate system with the optical center of the camera lens as the origin, the X_c and Y_c axes are parallel to the x and y axes of the image coordinate system, and the Z_c axis is perpendicular to the image plane.

$$\begin{Bmatrix} x \\ y \\ 1 \end{Bmatrix} = \frac{1}{Z_c} \begin{Bmatrix} f & 0 & 0 & 0 \\ 0 & f & 0 & 0 \\ 0 & 0 & 1 & 0 \end{Bmatrix} \begin{Bmatrix} X_c \\ Y_c \\ Z_c \\ 1 \end{Bmatrix}. \tag{2}$$

Among them, f is the focal length of the camera.

By synthesizing equations (1) and (2), equation (3) can be obtained, where matrix A contains 5 in-camera parameters $(k \ \ l \ \ u_0 \ \ v_0)$.

$$\begin{Bmatrix} u \\ v \\ 1 \end{Bmatrix} = \frac{1}{Z_c} \begin{Bmatrix} \frac{f}{k} & 0 & u_0 & 0 \\ 0 & \frac{f}{l} & v_0 & 0 \\ 0 & 0 & 1 & 0 \end{Bmatrix} \begin{Bmatrix} X_c \\ Y_c \\ Z_c \\ 1 \end{Bmatrix} = \frac{1}{Z_c} A \begin{Bmatrix} X_c \\ Y_c \\ Z_c \\ 1 \end{Bmatrix}. \tag{3}$$

The object coordinate system is the object's CAD Cartesian coordinate system established according to the CAD three-dimensional design drawing. The conversion relationship between the camera coordinate system and the object coordinate system is the following formula [10]:

$$\begin{Bmatrix} X_c \\ Y_c \\ Z_c \\ 1 \end{Bmatrix} = \begin{Bmatrix} R_{3\times3} & t_{3\times1} \\ 0^T & 1 \end{Bmatrix} \begin{Bmatrix} X \\ Y \\ Z \\ 1 \end{Bmatrix}. \tag{4}$$

Among them, $R_{3\times3} = (r_x r_y r_z)$ and $t_{3\times3} = (t_x t_y t_z)^T$ are the three undetermined rotation matrices and three undetermined translation vectors between the object coordinate system and the camera coordinate system, $0 = (000)^T$. The mapping relationship $k\tilde{m} = A(Rt)\tilde{M}$ between the object coordinate system and the image coordinate system can be obtained from (3) and (4), where $\tilde{m} = (uv1)^T$ is the homogeneous coordinate of the image, $\tilde{M} = (XYZ1)^T$ is the homogeneous coordinates of the object designed by CAD, and k is the scale coefficient. In order to solve the above 11 parameters, we select at least 6 sets of 2D and 3D point pairs (whose object coordinates and image coordinates are known) and list 11 equations according to formulas (3) and (4) to solve the above 11 unknown internal and external parameter, thereby the conversion relationship between the object coordinate system and the camera coordinate system

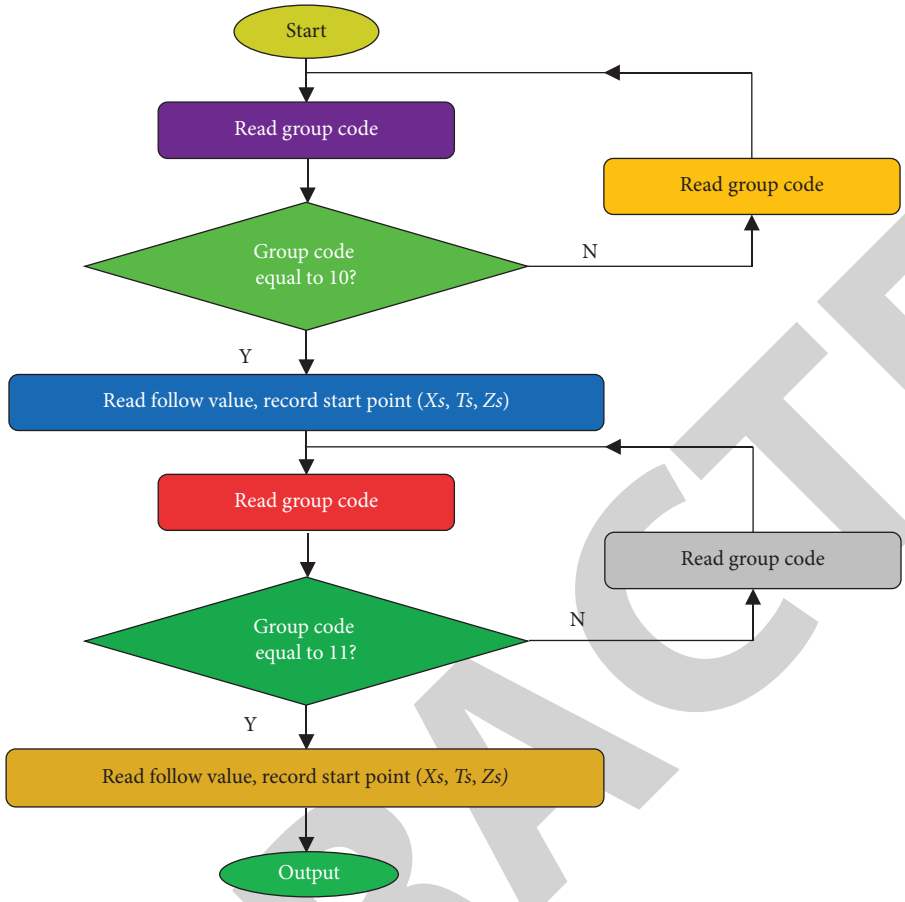

Figure 3: Flow chart of extraction of straight line entities.

is determined. When there are redundant observations, the unknown parameters can be solved by the least squares method [11]. We obtain a linear equation system of three equations containing the following three unknowns: $x1$, $x2$, and $x3$, the solved $x1$, $x2$, and $x3$ are the optimal solutions in the sense of least squares.

3.1.2. Getting the Initial Value. To establish a 3D coordinate system, we manually select 6 points ①–, and collect their 3D coordinates; to establish a coordinate system with the upper left corner of the image as the origin, we collect the two-dimensional image coordinates corresponding to ①–⑥; from the mapping relationship $k\tilde{m} = A(Rt)\tilde{M}$ between image coordinates and object coordinates (CAD design coordinates), the conversion parameters between the two-dimensional image coordinate system and the three-dimensional object coordinate system can be obtained [12].

By analyzing the DXF file structure of CAD graphics, the corresponding line entity information can be extracted. In the line entity data, the coordinates of the starting point of the line are the corresponding following values after group codes 10, 20, and 30, and the coordinates of the endpoint are the corresponding following values after group codes 11, 21, and 31. In the extraction process of straight line entities, we first determine whether the group code is 10. If so, we indicate that the following group value is the coordinate X_s of the starting point of the straight line, and similarly, we read the coordinates Y_s and Z_s of the point and the coordinates X_e, Y_e, and Z_e of the endpoint. We project (transform) the extracted straight line entity onto the image according to the transformation parameters and use this projection value as the initial value of the least squares template matching. Since the straight lines on the components may occlude each other, it is necessary to eliminate the lines that occlude each other, that is, the blanking process [13]. The specific steps of the straight line entity are shown in Figure 3.

The abovementioned process is adopted and the effect of obscuring straight lines is eliminated. The white line in the figure is the initial value range of the projection.

3.2. Line Segment Least Squares Template Matching. Least squares image matching (LSM) was proposed by Professor Ackermann in Germany [14]. LSM makes full use of the information in the image window to perform adjustment calculations so that the image matching can achieve an accuracy of 0.1 or even 0.01 pixels [15]. Gruen and Liu extended the LSM to use the given feature pattern as a reference template to perform least squares image matching with the actual image, so as to extract the target with high accuracy. It is called the least squares template matching (LSTM) method.

We set the gray level of the given target template as $g_m(x, y)$ and the actual image gray level as $g(x, y)$ and establish the matching of the two means $g_m(x, y) = g(x, y)$, that is, the gray value of each point in the target template is equal to the gray value of the corresponding point in the actual image. Due to the presence of noise, they cannot be completely equal in real images. Then, there is a difference between the template and the image, as follows [16]:

$$g_m(x, y) - v(x, y) = g(x, y). \tag{5}$$

The error equation of image matching is the following formula:

$$-v(x, y) = g_x(x, y)d_x + g_y(x, y)d_y + [g(x, y) - g_m(x, y)]. \tag{6}$$

By solving d_x and d_y between the initial position and the edge point, the precise location of the line edge can be obtained.

The basic idea of subpixel level line extraction is as follows: after image preprocessing, the CAD design data are first converted to parameters (projection) to obtain the initial value of the straight line segment of the image, and an adaptive straight line edge template is generated based on the initial value. The template matching is performed based on the principle of least squares. Finally, the least squares method is used for fitting, and the most or parameters $\widehat{k}$ and $\widehat{b}$ of the straight line equation are obtained. Line edge templates can be set to different templates according to different types of extracted edges [17, 18]. In this experiment, the feature extraction of the step profile is taken as an example, and the specific algorithm steps are as follows:

(i) Determination of the initial value range: we assume that the coordinates of the starting point and the endpoint of the initial value range of the straight line segment of the image obtained by projection are (x_1^0, y_1^0) and (x_2^0, y_2^0), respectively.

(ii) We generate an adaptive line-edge template. Let the known target line feature template be a small (Patch) image with a size of (5×5). The slope k of the straight line is given by the endpoints determined above through the midpoint of the image (3×3), and the grayscale value of the template is 0~255. According to the value of k, the template is gradually generated according to 5 grayscale levels.

(iii) We set the slope of the initial value line to be k, which is the initial position of $(x_1^0 + \Delta x, y_1^0 + \Delta y)$ matching, among them, $\Delta x = 1$, $\Delta y = k$, the target template, and the actual image generated between $(x_1^0 + \Delta x, y_1^0 + \Delta y - M)$ and $(x_1^0 + \Delta x, y_1^0 + \Delta y + M)$ (M is 1/2 of the template height) are based on $\sum vv = \min$ as the criterion, and perform least squares template matching to determine d_y. We record the best-fit point as (x_1, y_1), where $x_1 = x_1^0 + \Delta x$, $(d_y = \Delta x)$, and $y_1 \in (y_1^0 + \Delta y - M, y_1^0 + \Delta y + M)$.

(iv) repeat the above steps and use the method based on the least squares principle to perform template matching in the range $(x_1^0 + 2\Delta x, y_1^0 + 2\Delta y - M)$ and $(x_1^0 + 2\Delta x, y_1^0 + 2\Delta y + M)$ again and get the next best fit (x_2, y_2), until $x_1^0 + n\Delta x \geq x_2^0$. The point sequence (x_1, y_1), $(x_2, y_2) \ldots (x_n, y_n)$ is thus obtained.

It should be noted that, when $|k| \leq 1$, $\Delta x = 1$, $\Delta y = |k| \leq 1$; when $|k| > 1$, $\Delta x = 1$, $\Delta y = |k| > 1$. In order to make the matched point sequence denser, when $|k| \leq 1$, we match $(\Delta x = 1, \Delta y = k)$ along the x direction; when $|k| > 1$, the strategy of matching $(\Delta x = 1/k, \Delta y = 1)$ is performed along the y direction.

(v) Least squares straight line fitting: the least squares method is used to fit the point sequence generated by the above method, and the most or parameters $\widehat{k}$ and $\widehat{b}$ of the straight line equation are solved.

Let the equation of the straight line be the following formula:

$$\widehat{y} = \widehat{k}x + \widehat{b}. \tag{7}$$

According to the principle of least squares and the principle of the minimum sum of squares of deviations between y_i and $b + kx_i$, the following formula can be obtained:

$$\widehat{k} = \frac{\sum_{i=1}^{n}(x_i - \overline{x})(y_i - \overline{y})}{\sum_{i=1}^{n}(x_i - \overline{x})^2}, \qquad \widehat{b} = \overline{y} - \widehat{k}\overline{x}. \tag{8}$$

Among them, $\overline{y} = (1/n)(y_1 + y_2 + \cdots\cdots + y_n)$; $\overline{x} = (1/n)(x_1 + x_2 + \cdots\cdots + x_n)$.

In order to suppress image noise and improve the accuracy of line positioning, a second fitting can be performed on the fitted line, that is, after the first fitting, the matched point sequence is brought into the fitting result formula, and we calculate the residuals for each point. Then, some points with larger residual errors are removed, and the remaining points are fitted a second time. This process can be repeated several times until the mean square error is less than a certain threshold, the parameters of the new straight line equation are $\widehat{k}_1$ and $\widehat{b}_1$.

(vi) substitute the initial values x_1^0 and x_2^0 into the new straight line equation to obtain new endpoints (x_1^0, y_1') and (x_2^0, y_2'). Using this new endpoint as a new initial value, we repeat the above steps (ii) to (v) until the difference between the two adjacent sums is less than a certain threshold. We obtain the maximum values or values $\widehat{k}$ and $\widehat{b}$ of the extracted line parameters.

(vii) Finding the intersection of matching lines.

Let the equations of the extracted i-th and j-th straight lines be [19]

$$y = k_i x + b_i, y = k_j x + b_j. \tag{9}$$

The final intersection point coordinate (x, y) of the straight line can be solved by formula,

$$x = \frac{b_i + b_j}{k_i - k_j}, \quad y = \frac{b_i k_j + b_j k_i}{k_i - k_j}. \tag{10}$$

4. Analysis of Results

In order to test the accuracy of the straight line extracted by the algorithm in this paper, high-precision line feature extraction was carried out on the real image of a regular industrial part. The CAD data of regular industrial parts are provided by the design unit, 6 sets of 2D and 3D point pairs are obtained manually, and 11 projection transformation parameters are solved by the principle of least squares. According to the initial value range given by the projection transformation parameters, the straight line segment is accurately extracted by the adaptive least squares template matching method. Curve fitting is a very important descriptor in image analysis. The most commonly used curve fitting method is the least squares method. However, the general least squares method has certain limitations, and many scholars have made some improvements to it. Further, the least squares method is improved, and a new piecewise straight line fitting algorithm is proposed to replace the polynomial curve fitting in order to simplify the establishment of mathematical models and reduce the calculation so that it can better fit the point sequence.

Manual selection of two-dimensional and three-dimensional point pairs will inevitably lead to errors, so that the projected line has a certain projection error, but this projection value is only used as the initial value for high-precision extraction [20]. Using the initial value white line of the straight line obtained by projection conversion, the maximum errors of the projection point are 2.9 pixels and 3.3 pixels, respectively. It should be noted that in order to prevent the projection error from being too large, while ensuring the accuracy of manual measurement, the selected two-dimensional and three-dimensional points are relatively uniformly distributed around the object, and at the same time, the selected points are avoided on the same object plane [21]. This method can better solve the initial value problem of high-precision image feature extraction and the instability problem of image feature extraction caused by uneven image illumination. At the same time, the adaptive method is used to generate the matching template, which provides a guarantee for the automation of the method.

A stereo pair of industrial parts is acquired from different angles. Using the author's method, the image line feature renderings of the stereo image pairs are extracted, respectively.

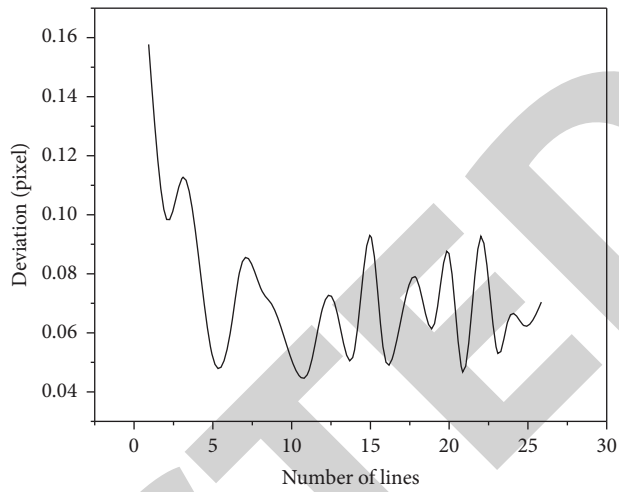

Figure 4: Standard deviation of straight line extraction (1).

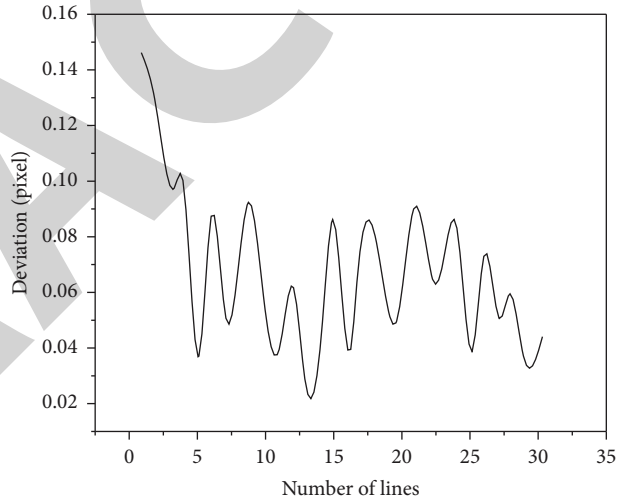

Figure 5: Standard deviation of straight line extraction (2).

In order to test the accuracy of the extracted straight line, the author evaluates it from two aspects: theoretical accuracy and practical accuracy.

(i) Theoretical accuracy: the standard deviation of the fitted straight line is an important sign to test whether the fitting result is valid. According to the deviation estimate of the least square fitting, the standard deviation of the fitted straight line is calculated according to formula [22, 23]:

$$S = \sqrt{\frac{1}{N-2} \sum_{i=1}^{N} \left[y_i - \left(\hat{b} + \hat{k} x_i \right) \right]^2}. \tag{11}$$

Among them, N is the number of fitting points and (x_i, y_i) are the coordinates of fitting points. The theoretical accuracy of straight line extraction is shown in Figures 4 and 5.

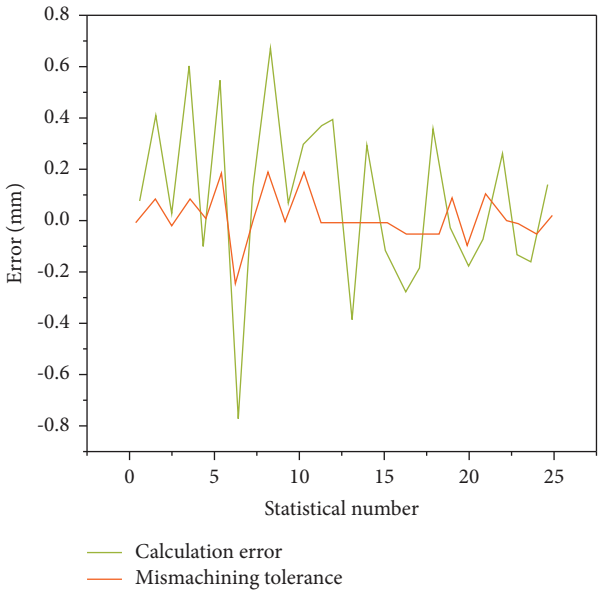

Figure 6: Statistical diagram of machining error and calculation error.

(ii) According to the straight line feature of the same name of the extracted stereo pair, using the internal and external parameters of the camera that have been checked and calibrated, we adjust (reconstruct) the object coordinates of the industrial parts and calculate the length of the straight line of the object based on this object coordinate (calculated length). Also, we measure the straight line length (measurement length) corresponding to the actual industrial parts and compare the results of manual measurement and adjustment calculation [24]. The "measured length" is the length of the straight line measured by the vernier caliper, and the "calculated length" is the corresponding straight line length calculated with the coordinates of the object. The "calculation error" in the table represents the difference between the calculated length and the measured length.

Statistical analysis of the experimental results showed that the median error of the difference between the calculated length and the measured length was 0.232 mm [25]. The "machining error" is calculated from the design length and the measured length of the part. Figure 6 is an image statistical representation of the machining error and the calculation error.

5. Conclusion

In order to extract image line features with high precision and realize vision-based image measurement, the author adopts the adaptive least squares line template matching method. By establishing the transformation relationship between the image coordinate system and the object CAD coordinate system, the CAD design coordinates are projected onto the image and taking this as the initial value for least squares template matching and fitting, therefore, the image line features are obtained with high precision, and the median error of the difference between the reconstructed line length and the length of the line measured by the vernier caliper is 0.232 mm. Linear feature extraction experiments on real images show that this method can better solve the initial value problem of high-precision image feature extraction and the image feature extraction instability problem caused by uneven illumination of the image. At the same time, an adaptive method is used to generate the matching template, which provides a guarantee for the automation of the method. The results of this study can be applied to high-precision image measurement and reverse engineering technology of regular industrial parts, which can help improve the automation level of industrial production. The high-precision extraction of circles and regular curves in industrial parts images will be the focus of the next step of this research.

The current retrieval system often has high retrieval speed but low retrieval accuracy. On the contrary, retrieval accuracy is high, but retrieval calculation time is very long. Therefore, the retrieval system cannot satisfy the user's requirement for a fast and good search model at the same time. Specifically, in terms of algorithms, simple descriptions, such as shape distribution descriptors, are designed, but in order to obtain more accurate matching results, the matching algorithm is more complicated, which increases the computational cost and sacrifices retrieval efficiency. However, if the descriptor is complex, that is, in order to extract more information and more complex shape features, such as descriptors that combine multiple shape features, it will take time to extract complex features, which will also bring about the problem of low retrieval efficiency. Therefore, it is necessary to find an effective descriptor and matching strategy framework, so that after offline training in the library, it can be quickly matched with the query model.

Data Availability

The data used to support the findings of this study are available from the corresponding author upon request.

Conflicts of Interest

The authors declare that they have no conflicts of interest.

References

[1] J. Rajeswari, J. Raja, and S. Jayashri, "Gradient contouring and texture modelling based cad system for improved tb classification," *Automated Software Engineering*, vol. 29, no. 1, pp. 1–12, 2022.

[2] R. V. Espinoza, K. C. Haatveit, S. W. Grossman, Y. T. Jin, and D. H. Sherman, "Engineering p450 tami as an iterative biocatalyst for selective late-stage c-h functionalization and epoxidation of tirandamycin antibiotics," *ACS Catalysis*, vol. 11, no. 13, 2021.

[3] F. Rasheed, M. Rommel, G. C. Marques, W. Wenzel, M. B. Tahoori, and J. Aghassi-Hagmann, "Channel geometry scaling effect in printed inorganic electrolyte-gated

transistors," *IEEE Transactions on Electron Devices*, vol. 68, no. 4, 2021.

[4] S. Gao and L. K. Bhagi, "Design and research on caddcam system of plane based on nc machining technology," *Computer-Aided Design and Applications*, vol. 19, no. 2, pp. 64–73, 2021.

[5] L. Ignaczak, G. Goldschmidt, C. A. D. Costa, and R. D. R. Righi, "Text mining in cybersecurity a systematic literature review," *ACM Computing Surveys*, vol. 54, no. 7, pp. 1–36, 2022.

[6] P. Cardaliaguet and N. Forcadel, "From heterogeneous microscopic traffic flow models to macroscopic models," *SIAM Journal on Mathematical Analysis*, vol. 53, no. 1, pp. 309–322, 2021.

[7] A. Chahi, Y. El merabet, Y. Ruichek, and R. Touahni, "Cross multi-scale locally encoded gradient patterns for off-line text-independent writer identification," *Engineering Applications of Artificial Intelligence*, vol. 89, Article ID 103459, 2020.

[8] Y. Feng, X. Tao, and E. J. Lee, "Classification of shellfish recognition based on improved faster r-cnn framework of deep learning," *Mathematical Problems in Engineering*, vol. 2021, no. 28, Article ID 1966848, 10 pages, 2021.

[9] M. Kamankesh, A. Mollahosseini, A. Mohammadi, and S. Seidi, "Haas in grilled meat: determination using an advanced lab-on-a-chip flat electromembrane extraction coupled with on-line hplc," *Food Chemistry*, vol. 311, Article ID 125876, 2020.

[10] X. Wei, D. Wei, D. Suo, L. Jia, and Y. Li, "Multi-target defect identification for railway track line based on image processing and improved yolov3 model," *IEEE Access*, vol. 8, 2020.

[11] H. Cai, H. Ma, and D. J. Hill, "A data-based learning and control method for long-term voltage stability," *IEEE Transactions on Power Systems*, vol. 35, no. 4, pp. 3203–3212, 2020.

[12] A. Arunan, T. Sirojan, J. Ravishankar, and E. Ambikairajah, "Real-time adaptive differential feature-based protection scheme for isolated microgrids using edge computing," *IEEE Systems Journal*, vol. 15, no. 1, pp. 1318–1328, 2021.

[13] D. Li, X. Wang, and Y. Yu, "Siamese visual tracking with deep features and robust feature fusion," *IEEE Access*, vol. 8, pp. 3863–3874, 2020.

[14] E. Petersen, J. Sauer, J. GraBhoff, and P. Rostalski, "Removing cardiac artifacts from single-channel respiratory electromyograms," *IEEE Access*, vol. 8, pp. 30905–30917, 2020.

[15] Z. Li, Q. Zhang, T. Long, and B. Zhao, "Ship target detection and recognition method on sea surface based on multi-level hybrid network," *Journal of Beijing Institute of Technology (Social Sciences Edition)*, vol. 30, pp. 1–10, 2021.

[16] X. Miao and Y. Liu, "Target recognition of sar images based on azimuthal constraint reconstruction," *Scientific Programming*, vol. 2021, no. 2, Article ID 9974723, 10 pages, 2021.

[17] X. Qian and D. Zhang, "A narrow deep learning assisted visual tracking with joint features," *Mathematical Problems in Engineering*, vol. 2020, no. 4, Article ID 8659890, 9 page, 2020.

[18] A. Sharma, R. Kumar, M. W. A. Talib, S. Srivastava, and R. Iqbal, "Network modelling and computation of quickest path for service-level agreements using bi-objective optimization," *International Journal of Distributed Sensor Networks*, vol. 15, no. 10, Article ID 155014771988111, 2019.

[19] S. Shriram, B. Nagaraj, J. Jaya, S. Shankar, and P. Ajay, "Deep learning-based real-time AI virtual mouse system using computer vision to avoid COVID-19 spread," *Journal of Healthcare Engineering*, vol. 2021, Article ID 8133076, 8 pages, 2021.

[20] X. Liu, C. Ma, and C. Yang, "Power station flue gas desulfurization system based on automatic online monitoring platform," *Journal of Digital Information Management*, vol. 13, no. 6, pp. 480–488, 2015.

[21] R. Huang, S. Zhang, W. Zhang, and X. Yang, "Progress of zinc oxide-based nanocomposites in the textile industry," *IET Collaborative Intelligent Manufacturing*, vol. 3, no. 3, pp. 281–289, 2021.

[22] Q. Zhang, "Relay vibration protection simulation experimental platform based on signal reconstruction of MATLAB software," *Nonlinear Engineering*, vol. 10, no. 1, pp. 461–468, 2021.

[23] S. Li, T. Xu, N. Jiang, H. Yang, S. Wang, and Z. Zhang, "Regional zenith tropospheric delay modeling based on least squares support vector machine using gnss and era5 data," *Remote Sensing*, vol. 13, no. 5, pp. 1004–1006, 2021.

[24] M. Said and O. Taouali, "Improved dynamic optimized kernel partial least squares for nonlinear process fault detection," *Mathematical Problems in Engineering*, vol. 2021, Article ID 6677944, 16 pages, 2021.

[25] J. Yuan, S. An, X. Pan, H. Mao, and L. Wang, "A wave peak frequency tracking method based on two-stage recursive extended least squares identification algorithm," *IEEE Access*, vol. 9, pp. 86514–86522, 2021.